IEEE Access
Multidisciplinary ⋮ Rapid Review ⋮ Open Access Journal

Received November 28, 2019, accepted December 23, 2019, date of publication December 27, 2019, date of current version January 14, 2020.

Digital Object Identifier 10.1109/ACCESS.2019.2962717

Multi-Agent-Based Voltage Regulation Scheme for High Photovoltaic Penetrated Active Distribution Networks Using Battery Energy Storage Systems

YONGXI ZHANG[1], (Member, IEEE), KE MENG[2], (Member, IEEE), FENGJI LUO[3], (Member, IEEE), HONGMING YANG[1], (Member, IEEE), JIAHUA ZHU[1], AND ZHAO YANG DONG[2]

[1]Energy Internet Driven by Big Data, National Base for International Science and Technology Cooperation, School of Electrical and Information Engineering, Changsha University of Science and Technology, Changsha 410114, China
[2]School of Electrical and Engineering and Telecommunications, University of New South Wales, Sydney, NSW 2052, Australia
[3]School of Civil Engineering, The University of Sydney, Sydney, NSW 2006, Australia

Corresponding author: Ke Meng (ke.meng@ieee.org)

This work was supported in part by the National Natural Science Foundation of China under Grant 51807011, and in part by the Hunan Provincial Natural Science Foundation of China under Grant 2018JJ3536.

ABSTRACT This paper develops a distributed voltage regulation scheme for high Photovoltaic (PV) penetrated distribution networks by utilizing battery energy storage (BES) units. In this study, multiple BES units form a multi-agent network, in which each BES unit acts as an individual agent and can communicate with its neighbors to perform the distribution network's voltage regulation in a cooperative manner. To cope with the uncertainties of PV power and load demand, a receding horizon-based approach is proposed, where BES control decisions for regulating bus voltages are updated with the update of the system's operational conditions (PV power, load, etc.). An efficient solving method – Distributed Alternating Direction Method of Multipliers Algorithm (D-ADMM) is applied to solve the proposed model under a colored network, where the BES agents with the same color synchronously update their states. Case studies are conducted on modified IEEE benchmark systems to validate the performance of the proposed method.

INDEX TERMS BES, distributed optimization, $l1$-norm regularization, multi-agent, receding horizon, voltage regulation.

I. INTRODUCTION

A. BACKGROUND

Photovoltaic (PV) solar power is one of the most promising renewable energy technologies in the world. The global PV market has been experiencing a tremendous growth. By 2018, the worldwide installed PV power capacity had reached 430GW [1]. PV integration can provide local production support to energy demands and relieve power Distribution Networks (DNs)' congestions. Nevertheless, due to its inherent stochastic nature, the integration of PV induces new challenges to the operation and control of DNs. One major challenge is the voltage rise problem that usually occurs in midday hours when solar radiation excesses the local demand. The redundant solar power would lead to rises of bus voltages, which consequentially would affect the grid's security and even cause physical damages to equipment [2].

B. RELATED WORK

To prevent the voltage rise problem, a variety of solutions have been proposed [3]–[5], including: (1) upgrade the grid, which is usually expensive and labour-intensive [3]; (2) utilization of voltage regulation devices such as fixed/switched capacitor banks and load tap changers [4]. Most of these devices are designed to operate in hourly basis time scale, and thus can hardly provide fast response to sudden changes of PV power [5]; (3) PV power curtailment, which is not preferable due to the waste of renewable energy [6].

Considering the high resistance/reactance (r/x) ratio in DNs, voltage magnitudes are sensitive to variations of active power. Therefore, an alternative solution for alleviating the voltage rise problem is to increase power consumption to accommodate the surplus solar power at some time intervals.

The associate editor coordinating the review of this manuscript and approving it for publication was Eklas Hossain.

This can be implemented through load management or using energy storage systems. Energy storage technologies have been rapidly developing in recent years. Currently there are different kinds of available energy storage techniques, including battery, fly-wheel, pumped hydro systems, compressed air energy storage, electrochemical double-layer capacitors (EDLCs), and so on. In the current market, compared with other energy storage systems, battery energy storage systems (BESS) is one of the most cost-effective ones due to its advantages of fast response time and high ramp rates. BES systems can be utilized to store excess PV energy and release it when there is a mismatch between power supply and consumption [7].

Numerous control strategies have been proposed in literature to deal with voltage fluctuation problems in DN, which can be classified into three types based on their architectures: 1) centralized, 2) decentralized; 3) multi-agent systems (MAS) based distributed control [8]. Centralized control techniques have been developed for controlling multiple BES units to regulate voltage in DNs in [6], [9]. However, centralized control scheme requires high investment in communication structure, which is vulnerable to external attacks and might cause information loss with limited bandwidth [10]. The second category is decentralized control method which only uses local information. References [11], [12] presented a coordinated control of PV and BESS for voltage regulation based on less complex communication infrastructure. However, due to the limited information sharing, it might induce frequency and voltage deviations which affect power quality [13].

Recently, MAS based distributed control for voltage regulation has attracted interests in academia [14]–[20]. Reference [15] proposes a two-stage voltage control scheme of dispersed DGs in a DN using the distributed Lagrangian primal dual sub-gradient algorithm. Reference [16] addresses the voltage regulation problem through the establishment of a rank-constrained semi-definite OPF model and a distributed solving approach. Reference [17] proposes a coordinated voltage control scheme in a low voltage distribution system, where a consensus algorithm is adopted for ESS active power output control. Reference [18] develops a hybrid method that combines both local droop control and distributed control to regulate the bus voltage profile. The method facilitates the effective operation of BESs under different conditions. In [19], a MAS based control strategy is developed to coordinate energy storage systems in a micro-grid, where the energy storage agents are organized into different groups to cooperatively regulate the micro-grid's voltage and frequency. In terms of considering communication time delays, [20] presents a distributed fixed-time MAS distributed control for BES and PV systems to perform voltage regulation and frequency restoration. However, most of above works [15]–[20] require all-to-all information exchange of agents; this can only be achieved either via a central controller or through a fully connected network topology, which limits their practical applications.

Moreover, aforementioned methods often perform real-time control in individually discrete time steps, and does not consider the coordination of control actions on a horizon covering multiple time steps [21]. This would often lead to solutions that are far away from optimal over a finite horizon. Further, existing works often do not consider the impact of frequent charging/discharging actions on BES's lifetime. In addition, most of these works do not consider the impact of forecasting errors of PV power and load.

C. CONTRIBUTIONS OF THIS PAPER

This paper proposes a MAS based control scheme for controlling BESs to regulate voltage for a DN with high PV penetration. The major contributions of this paper include following aspects:

1. Propose a voltage regulation model based on the cooperation of networked BESs. The $l1$-norm regularization is embedded in the model [22], [23] for finding the *minimum number* of BES units and *minimum actions* to all BES units to accomplish the voltage regulation task;

2. Propose a receding horizon strategy [24] to control the BESs to regulate voltage. The proposed strategy updates the system's operational condition with proceeding of time; based on this updated information, the control actions to the BESs are updated. In this way, the negative impact of the uncertain variables in the system's operation environment can be mitigated to a large extent;

3. Develop a D-ADMM [25]–[27] based approach for solving the proposed voltage regulation model. In the developed approach, voltage regulation is realized through limited information exchange among BES agents in a fully distributed manner.

The paper is organized as follows. Section II outlines the DN architecture and the multi-agent system. Section III presents the formulation of the voltage regulation problem. Section IV presents the distributed solving approach based on the D-ADMM algorithm. The effectiveness of the proposed method is examined via case studies in Section V. Section VI concludes the paper.

II. MULTI-AGENT SYSTEM STRUCTURE

A. SYSTEM STRUCTURE

Figure 1 depicts the conceptual architecture of a DN integrated with multiple BESs and PV generation sources. In this scenario, each BES unit is controlled by an Energy Management System (EMS) and acts as an independent agent. There is an underlying communication network that facilitates the communication among the BES units.

B. NOTATIONS AND NETWORK MODEL

Considering a DN integrating with H controllable BES agents that can communicate with each other. The DN can be modelled as an undirected graph $\mathcal{G} = \{\mathcal{V}, \varepsilon\}$, where $\mathcal{V} = \{1, 2, \cdots, H\}$ denotes the set of BES agents and $\varepsilon \subseteq \mathcal{V} \times \mathcal{V}$ is the set of edges. An edge connecting pairs of BESs

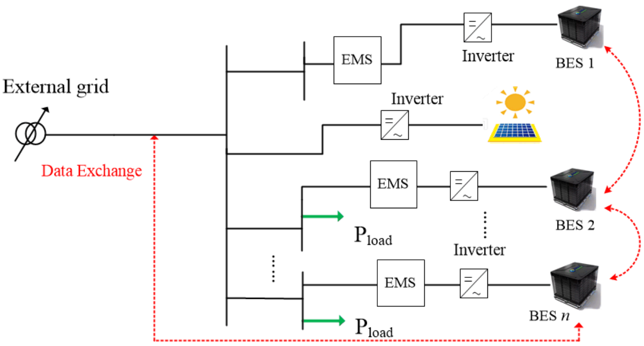

FIGURE 1. Conceptual architecture of the radial DN with PV and distributed BES units.

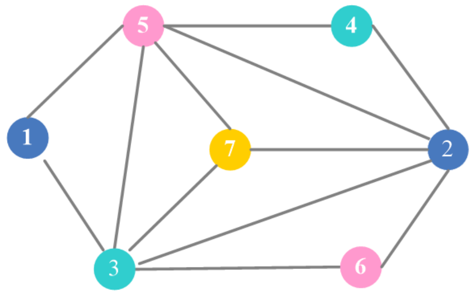

FIGURE 2. Example of colored MAS based framework.

that can communicate with each other. An edge (i, j) $(i, j \in \mathcal{V})$ connects BES agents i and j. The BES agents connected with the ith BES agent is known as the ith BES's neighborhood, whose set is denoted as $\mathcal{H}_i = \{j : (i, j) \in \varepsilon\}$. The degree of BES agent i (denoted as D_i) is defined as the cardinality of $|\mathcal{H}_i|$, i.e. $D_i = |\mathcal{H}_i|$.

We consider that the BES agents in the network are colored by L different colors, such that two neighboring BESs never share the same color. The first C_1BES agents are assigned with color *1* and are denoted as the set of $\mathcal{C}_1 = \{1, 2, \cdots, C_1\}$. The rest BES agents are colored in a same way. C_l BES agents marked in color l are counted denoted $\mathcal{C}_l = \{C_{l-1} + 1, \cdots, C_{l-1} + C_l\}$, and there is $|\mathcal{C}_1| + |\mathcal{C}_2| + \cdots + |\mathcal{C}_l| = H$. Figure 2 illustrates an example of a colored network, which comprises 7 agents and 12 edges. The agents are assigned with 4 different colors. The colored agents are divided to following four groups:

- $\mathcal{C}_1 = \{1, 2\}, |C_1| = 2; \mathcal{C}_2 = \{3, 4\}, |C_2| = 2;$
- $\mathcal{C}_3 = \{5, 6\}, |C_3| = 2; \mathcal{C}_4 = \{7\}, |C_4| = 1.$

III. VOLTAGE REGULATION PROBLEM FORMULATION

A. MODELING OF PV AND LOAD UNCERTAINTIES

Voltage regulation tasks in DNs are usually based on prediction of PV solar power and power demand. The prediction models used in this study are presented as below.

1) SOLAR POWER PREDICTION MODEL

Assuming PV array is equipped with a MPPT controller. The solar power generated by PV array are predicted as [28]:

$$P_{PV}(t) = f_{PV} P_{PV\_r} \frac{G(t)}{G_{STC}} [1 + \alpha_T (T(t) - T_{STC})] \tag{1}$$

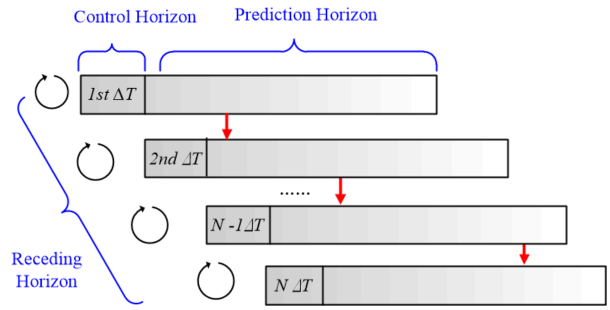

FIGURE 3. Proposed multi-step receding horizon update scheme.

where $P_{PV}(t)$ denotes PV output power at time t; P_{PV_r} is the rated output power of PV array, f_{PV} is the de-rating factor considering shading, wiring losses and snow cover, *etc*. G_{STC} and T_{STC} are the solar radiation and temperature on PV array under standard conditions. $G(t)$ and $T(t)$ are the solar radiation and temperature in current time, and α_T is the temperature coefficient of power. $G(t)$ represents the predicted solar radiation at time t, calculated as:

$$G(t) = \overline{G(t)} + \mu G(t) \tag{2}$$

where $\overline{G(t)}$ denotes the estimated solar irradiance; $\mu G(t)$ represents the estimation error that is assumed to follow a zero-mean Gaussian distribution.

2) POWER DEMAND PREDICTION MODEL

The predicted power load $P_{load}(t)$ at time t (kW) is calculated:

$$P_{load}(t) = \bar{P}_{load}(t) + \delta_{load}(t) \tag{3}$$

where $\bar{P}_{load}(t)$ and $\delta_{load}(t)$ are the estimated load value and estimation error. The estimation error is assumed to follow a truncated normal distribution with zero mean and the standard deviation of 5% [29].

B. RECEDING HORIZON BASED VOLTAGE CONTROL

PV power prediction accuracy would decrease with the increase of the prediction time horizon. To better handle the unavoidable prediction error, a receding horizon approach is applied in this study for voltage regulation. That is, in the first time step, the solar and load data are predicted for the while horizon (i.e. T time steps). Then, a voltage regulation model covering all the remaining T time steps is formulated (will be presented in Section IV) and solved. Only the control actions of the first ΔT time steps are actually applied to the BESs. When the time proceeds to the $\Delta T + 1$th time step, the solar & load prediction is re-performed for the next T time steps, the voltage regulation model is re-formulated and solved, and the control actions of the next ΔT time steps are applied. This process repeat until the end of the whole horizon is reached (Figure 3).

In each round of the receding horizon, a voltage regulation model is formulated and solved. The model determines: (1) which BESs from the BES network are selected to control;

and (2) how much power are charged/discharged to them. The objective function of the voltage regulation model is represented as Eq. (4). It aims to find *minimum number* of BES units and *minimum actions* of all BES units while satisfying the voltage constraints over the whole control horizon.

$$\min \sum\nolimits_{\forall i} f\left(\mathrm{P}_i\right) \tag{4}$$

$$f\left(P_i\right) = \sum\nolimits_{i} \|\mathrm{P}_1 +, \ldots + \mathrm{P}_i\|_1, \quad \forall i \in H \tag{5}$$

The decision variable P_i refers to the ith BES's power output; $\mathrm{P}_i = \left[P_{ch/dis,i}\left(1\right), P_{ch/dis,i}\left(2\right), \ldots P_{ch/dis,i}\left(t\right)\right]^{\mathrm{T}} \in \mathbb{R}^T$. $P_{ch/dis,i}\left(t\right)$ refers to the charging/discharging power of the ith BES at time t. H is the sets of buses with BESs installed. Eq. (5) represents the $l1$-norm expression of the objective function, which ensures sparsity of P_i (i.e. with least numbers of nonzero entries).

Model (4) is subjected to following constraints,

(1) BES operation constraints:

$$0 \leq P_{ch,i}\left(t\right), \quad \left|P_{dis,i}\left(t\right)\right| \leq P_{i,\max}^{bat}, \ \forall i \in H, \ \forall t \in T \tag{6}$$

$$E_{i,\min} \leq E_i\left(t\right) \leq E_{i,\max}, \quad \forall i \in H, \ \forall t \in T \tag{7}$$

$$E_i\left(t+1\right) = E_i\left(t\right) + \left(P_{ch,i}\left(t\right)\eta_{ch} - P_{dis,i}\left(t\right)/\eta_{dis}\right)\Delta t, \quad \forall i \in H, \quad t \in T \tag{8}$$

where T and Δt are the total number of time steps over the whole control horizon and the duration of each time step, respectively; $E_i\left(t\right)$ is to the ith BES's energy level at time t; $P_{i,\max}^{bat}$ denotes the ith BES's rated power; $E_{i,\min}$ and $E_{i,\max}$ are lower and upper limits of ith BES agent energy capacity; η_{ch} and η_{dis} refers to the BES's charging/discharging efficiency, respectively. Constraint (6) restricts the ith BES's power output cannot exceed its power capacity. Constraints (7)-(8) restrict the energy stored in the ith BES must be within an allowable range, so as to protect the BES from over charged/discharged and prolong its lifetime.

(2) Bus voltage constraints:

$$v_{n,\min} \leq v_{\mathrm{n}}\left(t\right) \leq v_{n,\max}, \quad \forall n \in N, \ \forall t \in T \tag{9}$$

where N denotes the set of system buses; $v_{n,\min}$ and $v_{n,\max}$ are lower and upper voltage limits for bus n; Eq. (9) denotes the voltage constraints for all the system buses n at time t.

(3) Power balance constraints:

$$\sum_{i \in H} P_{ch/dis,i}\left(t\right) + \sum_{i \in M} P_{PV,i}\left(t\right) + P_{ext}\left(t\right) = P_{load}\left(t\right), \quad \forall t \in T \tag{10}$$

where M is the sets of buses with PV sources. It is assumed that the DN operator can purchase electricity from the external grid. $P_{ext}\left(t\right)$ denotes the purchased power at time t.

(4) PV power constraints:

$$0 \leq P_{PV,i}\left(t\right) \leq P_{PV\_r,i}, \quad \forall i \in M, \ \forall t \in T \tag{11}$$

where $P_{PV\_r,i}$ denotes the rated power capacity of the ith PV source.

C. SENSITIVITY MATRIX

The influence of BES power outputs and bus voltage are calculated as below. Firstly, the relationship between power output and voltage can be expressed through Jacobian sensitivity matrix derived from the Newton-Raphson power flow calculation [30]. More specifically, the general conversion form between small variations in the system's active and reactive power output (ΔP and ΔQ) and the variations in phase angles and voltage ($\Delta\theta$ and ΔV) profile can be described as:

$$\begin{pmatrix} \Delta\theta \\ \Delta V \end{pmatrix} = \begin{pmatrix} \Lambda_{\theta P}\Lambda_{\theta Q} \\ \Lambda_{VP}\Lambda_{VQ} \end{pmatrix} \begin{pmatrix} \Delta P \\ \Delta Q \end{pmatrix} \tag{12}$$

Due to the high r/x ratio value in DN, changes in active power injections might significantly affect bus voltage variation (reactive power ΔQ injection has little effects and thus can be neglected). The voltage value at a time step can be approximately calculated based on the voltage at the previous time step, the Jacobian sensitivity matrix, and the active power output change ΔP:

$$\mathrm{V}_{t+1} = \mathrm{V}_t + \Lambda_{VP} \times \Delta P \tag{13}$$

D. RELAXED VOLTAGE CONSTRAINTS

Generally, a DN system's bus voltage variation is set to be within ±5% of the nominal value. Once the voltage of one or more buses fall out of the allowable range, the DN operator would need to bring voltage back to the secure range as soon as possible. However, in practical situations, the voltage is hardly to be regulated back to the secure rage in the first time. Therefore, a relaxation factor ξ is applied to all the system buses [31], to let the bus voltage can be regulated smoothly back to the secure range by the end of the control horizon ΔT.:

$$-\xi + v_{n,\min} \leq v_{\mathrm{n}}\left(t\right) \leq v_{n,\max} + \xi, \quad \forall n \in N, \ \forall t \in \Delta T \tag{14}$$

where $\xi = \xi^{\Delta \mathrm{T}}$ is the vector of slack variables.

IV. D-ADMM BASED SOLVING APPROACH

Considering the distributed nature of energy resources in DNs, it is impractical (or at least very difficult) for a controller to dispatch the large number of dispersed energy resources centrally. Thus, a MAS based distributed control scheme would be preferable for DN's voltage regulation. In this study, we develop a distributed control strategy to solve model (4)-(14). The control strategy is based on limited information exchange among neighboring BESs using specific communication protocols that were designed for parallel processing.

A. PROBLEM FORMULATION

The proposed model in Eq. (4)-(14) is the sum of separable convex objective functions with linear constraints. To apply D-ADMM, we decouple model (5) into the sum of individual objective functions related to each

BES agent:

$$\min_{\mathrm{P}_i=(\mathrm{P}_1,\ldots,\mathrm{P}_H)} \sum f_i(\mathrm{P}_i)$$
$$s.t.\ \mathrm{P}_i \in \mathcal{P}_i \quad \forall i \in H$$
$$\mathrm{P}_i = \mathrm{P}_j, \quad i,j \in \varepsilon \tag{15}$$

All constraints (6)-(11) and (14) are copied to each BES. $\mathrm{P}_i = (\mathrm{P}_1, \ldots, \mathrm{P}_H)$ represents the decision variables. Model (15) is solved in an iterative manner; in each iteration, each BES has individual objective function, and sends a copy of its solution to other BESs in the network. We use $\mathrm{P}_i \in \mathbb{R}^n$ to denote the copy hold by the BES i, which represents the solution of the whole BES network at the current iteration. $f_i(\mathrm{P}_i)$ refers to the separated local objective functions for the ith BES agent. $\mathrm{P}_i \in \mathcal{P}_i$ represents the feasible local variable set $\mathcal{P}_i$ for BES agent i. BES i only can access to its private objective function f_i and private set $\mathcal{P}_i$. $\mathrm{P}_i = \mathrm{P}_j$ for all BES agents i and j with edge $i, j \in \varepsilon$, which enforces all copies to be equal since the network is connected.

As presented in Section II.B, we assume the network topology is colored by L colors. BES agent s with color l are marked as C_l. There are colored sets $C_1, C_2, \ldots, C_l$ in total, with the cardinality of $C_l = |\mathcal{C}_l|$. Here $\{\mathcal{C}_l\}_{l=1}^{L}$ partitions $\mathcal{V}$. Therefore, problem (15) can be further converted as:

$$\min_{\overline{\mathrm{P}_l}} \sum_{l=1}^{L} f_i\left(\overline{\mathrm{P}}_l\right)$$
$$s.t.\ \overline{\mathrm{P}_l} \in \overline{\mathcal{P}_l}, \quad l = 1, 2, \ldots, L$$
$$\sum_{l=1}^{L} \left(D_l^T \otimes I_n\right)\overline{P_l} = 0 \tag{16}$$

$\overline{P_l} = \left(\overline{\mathrm{P}}_1, \cdots, \overline{\mathrm{P}}_l\right)$ ($\overline{\mathrm{P}}_l \in (\mathbb{R}^n)^L$) is copied to all the BESs with color l. There is $D = \left[D_1^{\mathrm{T}}, \cdots, D_L^{\mathrm{T}}\right]^{\mathrm{T}}$, where D is the arc-incidence matrix of the network topology; I_n is the identity matrix of dimension n; $\otimes$ denotes the Kronecker product. Each column of D is associated with an edge $(i, j) \in \varepsilon$. The ith and jth entry of D is with the value of either 1 or -1, and the rest entries are 0.

B. MAS VOLTAGE CONTROL BASED ON D-ADMM

Model (16) can be reformulated in the way of putting the decision variables of the same-colored BESs together to make the model be suitable for distributed implementation. Given L functions g_l, L sets P_l, and L sets of the full column rank matrix A_l:

$$\min_{\mathrm{P}_l} \sum_{l=1}^{L} g_l(\mathrm{P}_l)$$
$$s.t.\ \mathrm{P}_l \in \mathcal{P}_l, \quad l = 1, 2, \ldots, L$$
$$\sum_{l=1}^{L} A_l \mathrm{P}_l = 0 \tag{17}$$

where $\mathrm{P}_l = (\mathrm{P}_1,\ldots,\mathrm{P}_L)$ is the optimization variable; $A_l = D_l^{\mathrm{T}} \otimes I_n$ is the transported node-arc incidence matrix of the graph $\mathcal{G}$. Then, the original problem (model (4)-(14) is transferred to a color-based form. With this formulation, D-ADMM can be applied to solve the model.

Firstly, model (17) is rewritten to be the form of the augmented Lagrangian function with penalty terms:

$$L_\rho(\mathrm{P}_l, \lambda) = \sum_{l=1}^{L} \left(\sum g_l(\mathrm{P}_l) + \lambda^{k^{\mathrm{T}}} A_l \mathrm{P}_l\right) + \frac{\rho}{2}\left\|\sum_{l=1}^{L} A_l \mathrm{P}_l\right\|^2 \tag{18}$$

Here λ is the dual variable and ρ is a positive parameter. Using the D-ADMM algorithm, an iterative procedure can be applied to find the optimal value of P_l and λ:

$$\mathrm{P}_1^{k+1} = \arg\min_{\mathrm{P}_1 \in \mathcal{P}_1} L_\rho\left(\mathrm{P}_1, \mathrm{P}_2^k, \ldots, \mathrm{P}_L^k; \lambda^k\right) \tag{19}$$
$$\mathrm{P}_2^{k+1} = \arg\min_{\mathrm{P}_2 \in \mathcal{P}_2} L_\rho\left(\mathrm{P}_1^{k+1}, \mathrm{P}_2, \ldots, \mathrm{P}_L^k; \lambda^k\right) \tag{20}$$
$$\cdots\cdots$$
$$\mathrm{P}_L^{k+1} = \arg\min_{\mathrm{P}_L \in \mathcal{P}_L} L_\rho\left(\mathrm{P}_1^{k+1}, \ldots, \mathrm{P}_{L-1}^{k+1}, \mathrm{P}_L; \lambda^k\right) \tag{21}$$
$$\lambda^{k+1} = \lambda^k + \rho \sum_{l=1}^{L} A_l \mathrm{P}_l^{k+1} \tag{22}$$

where $i = 1, 2, ..., L$; k denotes the iteration number.

For BES agents with color l, the optimization problem of (19)-(22) is decomposed into $\mathcal{C}_l$ optimization problems that can be solved in parallel. In this way, the variable vector $\mathrm{P}_l = (\mathrm{P}_1, \mathrm{P}_2, \ldots, \mathrm{P}_L)$ is updated as:

$$\mathrm{P}_l^{k+1} = \arg\min_{\mathrm{P}_l \in \mathcal{P}_l} \sum_{i \in \mathcal{C}_l} f_i(\mathrm{P}_i) + \lambda^k A_l \mathrm{P}_i + \frac{\rho}{2}\left\|A_l \mathrm{P}_l + \sum_{i=1,..L,i\neq l} A_l \mathrm{P}_i^k\right\|^2 \tag{23}$$

The first two terms of Eq. (23) are linear combinations of the Lagrangian and relative to the agents with color l. The last term in Eq. (23) can be expressed as:

$$\frac{\rho}{2}\left\|A_l \mathrm{P}_l + \sum_{i=1,..L,i\neq l} A_l \mathrm{P}_i^k\right\|^2 = \frac{\rho}{2}\mathrm{P}_l^{\mathrm{T}} A_l^{\mathrm{T}} A_l \mathrm{P}_l + \rho \mathrm{P}_l^{\mathrm{T}} \sum_{i=1,..L,i\neq l} A_l^{\mathrm{T}} A_l \mathrm{P}_i^k + \frac{\rho}{2}\left\|\sum_{i=1,..L,i\neq l} A_l \mathrm{P}_i^k\right\|^2 \tag{24}$$

Because color-l agents are not connected with each other, $A_l^{\mathrm{T}} A_l$ is a diagonal matrix, in which the diagonal elements being the degree of the respective agent. Then, Eq. (24) can be simplified as:

$$\frac{\rho}{2}\left\|A_l \mathrm{P}_l + \sum_{i=1,..L,i\neq l} A_l \mathrm{P}_i^k\right\|^2 = \sum_{i \in \mathcal{C}_l} \frac{\rho G_i}{2} \|\mathrm{P}_i\|^2 - \rho \sum_{i \in \mathcal{C}_l} \sum_{j \in L} \mathrm{P}_i^{\mathrm{T}} \mathrm{P}_j^k + \frac{\rho}{2}\left\|\sum_{i=1,..L,i\neq l} A_l \mathrm{P}_i^k\right\|^2 \tag{25}$$

where $\lambda^k A_l \mathrm{P}_l = \sum_{i\in\mathcal{L}_l}\sum_{j\in\mathcal{H}_i}\lambda_{ij}^{k\,\mathrm{T}}\mathrm{P}_i$, λ_{ij} is defined for $i<j$ and associated with constraint $\mathrm{P}_i = \mathrm{P}_j$ in (17). The last term in (25) does not depend on P_l, and thus can be ignored. Then, Eq. (23) can be simplified as:

$$P_l^{k+1} = \underset{\overline{P}_l\in\overline{\mathcal{P}_l}}{\arg\min}\sum_{i\in\mathcal{C}_l} f_i(\mathrm{P}_i) + \left(\gamma_p^k - \rho\sum_{j\in\mathcal{H}_i} P_j^k\right)^T P_l + \frac{\rho D_i}{2}\|\mathrm{P}_i\|^2 \quad (26)$$

where $\gamma_i^k = \sum_{j\in\mathcal{H}_i}{}^{\lambda_{ij}^k}$ for local BES i. The auxiliary dual variable is expressed as:

$$v_i^k = \gamma_i^k - \rho\sum_{\substack{j\in\mathcal{H}_i\\ j<i}} P_j^{k+1} - \rho\sum_{\substack{j\in\mathcal{H}_i\\ j>i}} P_j^k \quad (27)$$

for $i\in\mathcal{C}_l$.

Then problem (27) is decomposed into $\mathcal{C}_l$ sub-problem and can be solved in parallel:

$$\mathrm{P}_i^{k+1} = \underset{\mathrm{P}_i\in\mathcal{P}_i}{\arg\min} f_i(\mathrm{P}_i) + \sum_{i\in\mathcal{H}_i} v_i^{k\,\mathrm{T}}\mathrm{P}_i + \frac{\rho G_i}{2}\|\mathrm{P}_i\|^2 \quad (28)$$

After the updates of P_i and dual variable γ_i^k of BES i, there is:

$$\gamma_i^{k+1} = \gamma_i^k + \rho\sum_{j\in\mathcal{H}_i}\left(\mathrm{P}_i^{k+1} - \mathrm{P}_j^{k+1}\right) \quad (29)$$

In the computation process, the ith BES receives charging/discharging information from all its neighbouring BESs with lower-order colours. After that, ith BES solves model (28); meanwhile, the BESs with the same colour update P_i individually. In this way, the parallel implementation improves the convergence speed.

C. OVERALL WORKFLOW OF MAS BASED VOLTAGE REGULATION

By applying the D-ADMM and receding horizon strategy, the overall showing in Eq. (18) and (26)-(29), the overall voltage regulation procedures are shown as follows:

It should be noted that, in the each optimization round of the receding horizon: 1) all the initial input data and system dynamic constraints must be adjusted; and (2) the dual variables should be set with zero at the end of the optimization.

Remark: With the communication topology of the BES network presented before, the D-ADMM algorithm is proven to strictly converge in [23].

Algorithm 1 (MAS Based Receding Horizon Voltage Regulation Control Scheme)

Initialization
1: **For** $t = 1: T$ do:
PV power and load demand prediction at every ΔT
Solve proposed problem over time horizon $[t, t+T]$:
2: I. Set: $k=1$,
Initialize: $\gamma_i^1 = 0$, $\mathrm{P}_i^1 = 0$ $(\forall i\in H)$.
4: **Repeat**:
5: [for $l = 1, 2, \ldots L$] do
6: [for $i\in\mathcal{C}_l$ in parallel] do
1) Update auxiliary dual variable according to (27).
2) BES Agent i with color l receives the variables from $j\in\mathcal{H}_i$, update optimal variables $\left\{\mathrm{P}_i^{k+1}\right\}_{i\in H}$ according to (28). Send updated value P_i^{k+1} to its neighbors.
7: **End**
8: **End**
3) For all $L\in\mathcal{V}$, update the dual variables according to (29) to obtain γ_i^{k+1}.
10: **End**
11: II. Set $k = k+1$ and return to Step I until a predefined stopping criterion is met.
12: **End**
Output: P_i, $i = 1, 2, \ldots, H$

V. CASE STUDY

A. SIMULATION SETUP

In this section, we report the results of the numerical simulation conducted for evaluating the performance of the proposed method. The simulation is implemented by YALMIP toolbox and MATLAB (version R2018a), and executed on a 3-GHz DELL PC with Intel i7-4790 3.60 GHz CPU and 8 GB RAM. We use the load and solar power data recorded in a typical summer day in south Australia [32], [33]. PV penetration level is set to be 50% during the peak load hours. The entire time horizon is set to be 2 hours (11pm-13pm) with the duration of each time step is 5 minutes (i.e. $\Delta t = 5$ min). The control horizon is 15 minutes. Hence, $\Delta T = 3$, $T = 24$ time steps. $\mathrm{P}_i \in \mathbb{R}^{24\times 1}$, where $\mathrm{P}_i(t)$ refers to the power of ith BES at the ith time step.

The simulation results of the proposed method in each iteration are compared with the optimal solutions, with the comparison difference calculated as:

$$\begin{aligned}\varepsilon(k) &= \left|\sum f_i\left(\mathrm{P}_i^k\right) - J_i\right| \Big/ J_i\\ x^{\mathrm{diff}}(k) &= \left|\mathrm{P}_i^k - x^*\right| \Big/ x^*\end{aligned} \quad (30)$$

where k is the iteration index; $f_i\left(\mathrm{P}_i^k\right)$ and P_i^k are objective function value and solutions of the D-ADMM control scheme, respectively; J_i and x^* denote the objective function value and solution obtained from the centralized optimization with receding horizon.

B. 15-BUS SYSTEM

We test our method on the modified IEEE 15-bus system, whose topology is shown in Figure 4. The network parameters of the system are available in [34]. The secure range of the voltage in each bus (excluding slack bus) is set as [0.95, 1.05] p.u. Two PV panels are located on buses 8 and 10 respectively; they can operate up to 0.9 power factor. Five BESs are installed at bus 4, 7, 9, 11, and 14. The relevant BES data are given in Table. 1 [35].

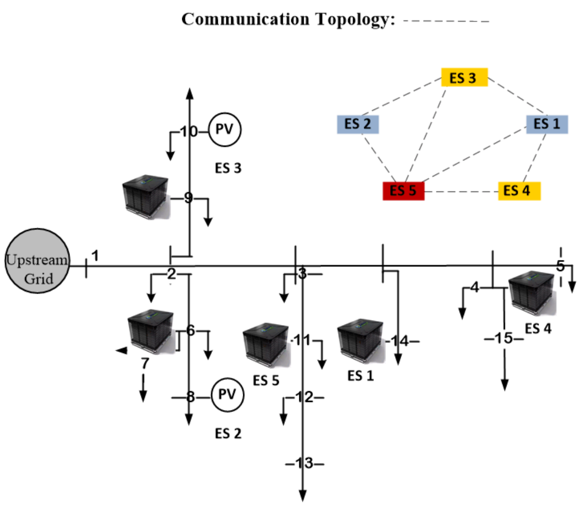

FIGURE 4. Communication network of modified 15-bus distribution system with five BES units, seven edges labeled in three colors.

TABLE 1. BES units technical data.

NO.	Power Capacity (MW)	Energy Capacity (MWh)	Technology	SOC limit
1	0.10	0.60	Lead-acid	
2	0.10	0.60	Lead-acid	
3	0.10	0.60	Zn/BR	0.2~0.8
4	0.10	0.60	Zn/Br	
5	0.05	0.30	Li-ion	

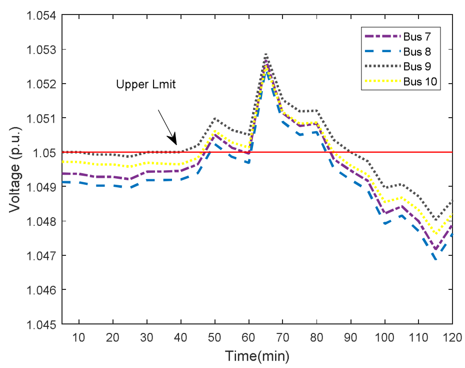

FIGURE 5. Voltage magnitudes for bus 7-10 during 11:00-13:00 pm.

We firstly analyze the simulation based on the PV and load profiles without considering forecasting errors. Figure 5 shows system voltage profile over the entire time horizon in buses 7-10. It can be observed that the voltages significantly violate the system voltage constraints at $t = 10$ and $t = 15$. With the relaxed voltage constraints, the system operator can mitigate the voltage rise issue smoothly through stepwise voltage regulation. As long as all the monitored bus voltage profiles are brought back to the secure range, the system does not further require any supports from the BESs. Figure 6 shows the detailed SOC profiles of all five BES agents over the entire control horizon.

Table 2 reports the BES power outputs under different values of the relaxation factor ξ. The relaxed voltage upper limits are 1.053 p.u. and 1.0515 p.u., and the voltage constraints

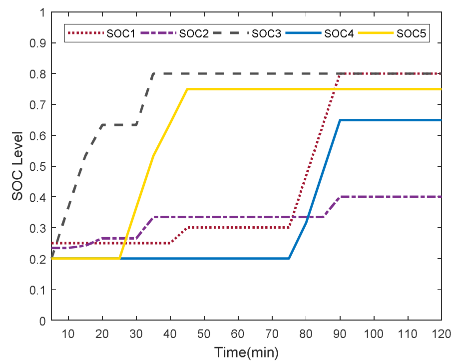

FIGURE 6. BES SOC profiles for the entire time horizon.

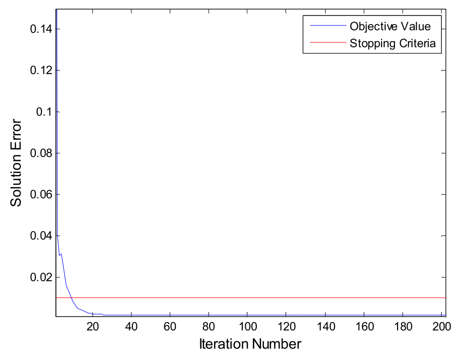

FIGURE 7. Objective function values comparison between centralized optimization and D-ADMM algorithm.

are decremented by 0.001 p.u. and 0.0005 p.u. per each time step in three time steps, respectively. It can be seen that when the value of ξ decreases, the involved numbers of BES agents increase and the amount of charging/discharging power increases as well. The relaxed voltage constraints provide proper correction of the voltage profiles especially under severe conditions. This allows the DN operator to adopt most suitable control actions to achieve a trade-off between security and effectiveness.

To analyze the convergence of the proposed method, Fig. 7 compares $\varepsilon(k)$ and $x^{\text{diff}}(k)$ of the results from D-ADMM and centralized optimization using the interior-point method, where the x-axis and y-axis represent the iteration numbers used to reach the same accuracy (pre-defined as 0.01) and the error of the objective function, respectively. The stopping criteria is set as 0.01. The proposed D-ADMM control scheme converges after 21 iterations, with the total time consumption of only 1.27 seconds. The results also show that through limited information exchange between the neighboring BESs, the same global optimized solution can be obtained by both centralized and distributed approaches.

We further compare the convergence performance of the D-ADMM based voltage regulation with the original ADMM based approach, and the results are shown in Figure 8, We can find that both of the two algorithms can guarantee the optimality of the solution, but the convergence speed of D-ADMM (21 iterations) is much faster than that of ADMM (41 iterations).

TABLE 2. Solutions under different values of ξ.

Time (min.)	ξ =0.001 pu/ time step					ξ = 0.0005 pu/ time step				
	ES1	ES2	ES3	ES4	ES5	ES1	ES2	ES3	ES4	ES5
5	0.10	0.09	0.10	0.10	0.05	0.10	0.09	0.10	0.10	0.05
10	-	-	0.03	-	-	-	0.01	-	-	-
15-20	-	-	-	-	-	-	-	-	-	-
25	-	-	0.03	-	-	-	-	0.06	-	-
30	0.03	-	0.10	-	0.05	-	0.01	0.10	-	0.02
35	0.10	-	0.10	-	0.05	0.08	-	0.10	-	0.05
40	0.10	-	-	-	0.02	0.10	-	-	-	0.04
45	-	-	-	-	-	-	-	-	-	-
50	-	-	-	-	-	-	0.02	-	-	-
55	-	-	-	-	-	-	-	-	0.06	-
60	-	-	-	-	-	0.04	-	-	0.10	-
65	-	-	-	-	-	-	-	-	0.10	-
70-80	-	-	-	-	-	-	-	-	0.06	-
85	-	-	-	0.07	-	-	-	-	-	-
90	-	0.02	-	0.10	-	-	-	-	-	-
95-120	-	-	-	-	-	-	-	-	-	-

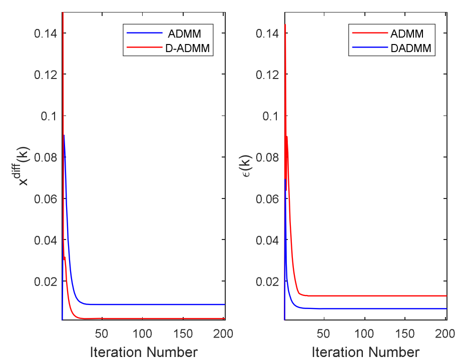

FIGURE 8. The dynamic convergence performance of the relative error in ADMM and D-ADMM (a) Independent variables; (b) objective function.

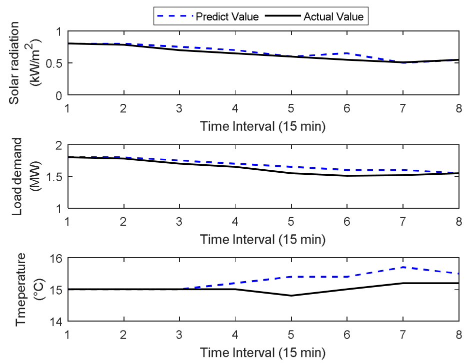

FIGURE 9. Temperature, load demand and solar radiation profiles within entire time horizon.

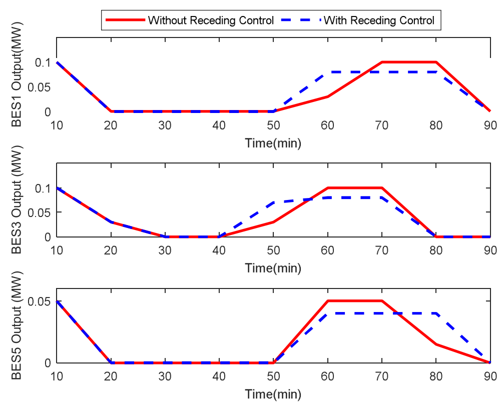

FIGURE 10. BES units output power with and without receding horizon control for the 15-bus system.

C. RESULTS ANALYSIS WITH PREDICTION UNCERTAINTIES

In this sub-section, effectiveness of the proposed receding horizon strategy on voltage regulation is evaluated, with taken into account the prediction errors of solar power and load. The load demand and solar radiation are predicted 2 hours ahead and the prediction is updated every 15 minutes. Figure 9 shows the predicted and actual profiles of load and solar irradiance respectively.

Figure 10 shows the BES power output profiles with and without using the receding horizon control approach. The red line indicates the control action plan without the receding horizon control approach; only the actions during the first 15 minutes are actually applied. The blue dash line denotes the corrected control scheme based on the receding horizon control. It can be observed that the BESs adapt to the updated environmental variables. With the proposed receding horizon control algorithm, the BESs output power are smoothed along whole control horizon. For example, for 1th, 3th and 5th BESs, The BES power output is smaller

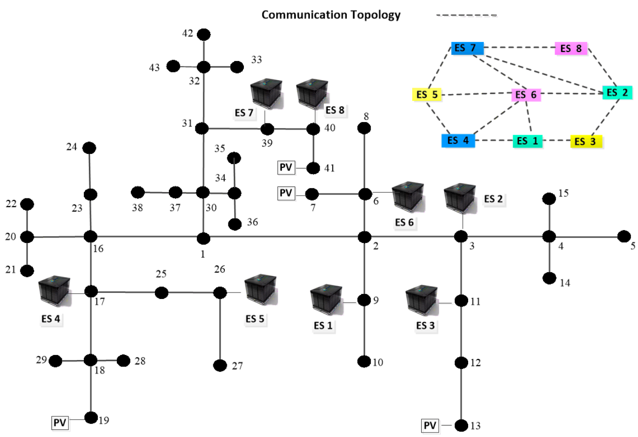

FIGURE 11. **Communication network of 43-bus distribution system with eight BES units, eleven edges labeled in four colors.**

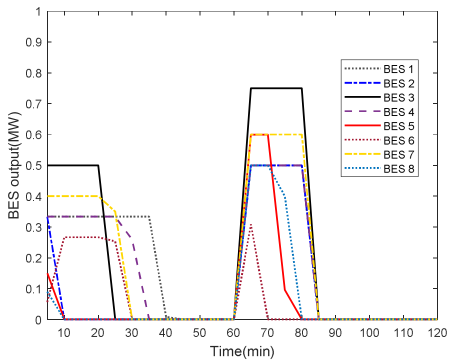

FIGURE 12. **BES output power for the 43 bus for the entire time horizon.**

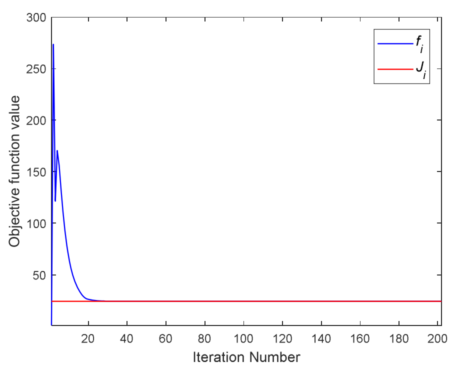

FIGURE 13. **Objective function values computed by the D-ADMM algorithm and centralized optimization.**

during time [50-80] minutes. The regulation converges to the new optimum with the update information.

D. 43-BUS DISTRIBUTION SYSTEM

In this case, we test our algorithm on a 43-bus system. The topology of the 43 bus is shown in Figure 11, where four PV panels are installed at buses 7, 13, 19, and 41. Eight BES units are installed at buses 9, 3, 11, 17, 26, 6, 39, and 40, respectively. Same with the previous case, the entire control horizon and the duration of each time step are set as 2 hours and 5 minutes, respectively.

Similarly, Figure 12 and 13 present the comparison of BES power output and the objective function value between the D-ADMM and centralized optimization approaches. From the results, we can find that each BES unit communicates with their neighbors and finally reached the optimal decision cooperatively. The decision variables for all BESs converges after several iterations and the objective function value reaches the optimality, same with that obtained by the centralized optimization.

VI. CONCLUSION AND FUTURE WORK

This paper proposes a MAS based voltage regulation framework in DNs with high PV penetration. The method controls the BES units' power output to mitigate the voltage rise issue in a distributed manner. To achieve this, the $l1$-norm is embedded in the objective function. The proposed method is mainly characterized by two features:

(1) it uses a receding horizon approach to continuously update the system's states and the control actions to the BESs. The simulation results on two modified IEEE benchmark systems show that the receding horizon strategy can well adjust the BESs' outputs while maintaining the bus voltages within the secure range;

(2) it uses a fully distributed control scheme based on D-ADMM algorithm for determining the charging/discharging control actions to the BESs. The simulation results show that the D-ADMM algorithm has a strong capability for performing global optimization and has faster convergence ability than the original ADMM algorithm.

Future works can be conducted in several directions. For example, a more comprehensive system structure can be studied by considering various kinds of voltage regulation devices such as inverter and capacitor banks. In addition, the penetration of reactive power optimization can be also considered for voltage regulation.

REFERENCES

[1] *Energy Australia*. Accessed: 2020. [Online]. Available: https://www.energyaustralia.com

[2] J. Tuominen, S. Repo, and A. Kulmala, "Comparison of the low voltage distribution network voltage control schemes," in *Proc. IEEE PES Innov. Smart Grid Technol., Eur.*, Istanbul, Turkey, Oct. 2014, pp. 1–6.

[3] R. A. Shayani and M. A. G. De Oliveira, "Photovoltaic generation penetration limits in radial distribution systems," *IEEE Trans. Power Syst.*, vol. 26, no. 3, pp. 1625–1631, Aug. 2011.

[4] A. Keane, L. F. Ochoa, E. Vittal, C. J. Dent, and G. P. Harrison, "Enhanced utilization of voltage control resources with distributed generation," *IEEE Trans. Power Syst.*, vol. 26, no. 1, pp. 252–260, Feb. 2011.

[5] A. Safavizadeh, G. R. Yousefi, and H. R. Karshenas, "Voltage variation mitigation using reactive power management of distributed energy resources in a smart distribution system," *IEEE Trans. Smart Grid*, vol. 10, no. 2, pp. 1907–1915, Mar. 2019.

[6] L. Wang, D. H. Liang, A. F. Crossland, P. C. Taylor, D. Jones, and N. S. Wade, "Coordination of multiple energy storage units in a low-voltage distribution network," *IEEE Trans. Smart Grid*, vol. 6, no. 6, pp. 2906–2918, Nov. 2015.

[7] T. Zhao and Z. Ding, "Distributed agent consensus-based optimal resource management for microgrids," *IEEE Trans. Sustain. Energy*, vol. 9, no. 1, pp. 443–452, Jan. 2018.

[8] K. E. Antoniadou-Plytaria, I. N. Kouveliotis-Lysikatos, P. S. Georgilakis, and N. D. Hatziargyriou, "Distributed and decentralized voltage control of smart distribution networks: Models, methods, and future research," *IEEE Trans. Smart Grid*, vol. 8, no. 6, pp. 2999–3008, Nov. 2017.

[9] M. J. E. Alam, K. M. Muttaqi, and D. Sutanto, "Mitigation of rooftop solar PV impacts and evening peak support by managing available capacity of distributed energy storage systems," *IEEE Trans. Power Syst.*, vol. 28, no. 4, pp. 3874–3884, Nov. 2013.
[10] G. Mokhtari, G. Nourbakhsh, and A. Ghosh, "Smart coordination of energy storage units (ESUs) for voltage and loading management in distribution networks," *IEEE Trans. Power Syst.*, vol. 28, no. 4, pp. 4812–4820, Nov. 2013.
[11] J. Von Appen, T. Stetz, M. Braun, and A. Schmiegel, "Local voltage control strategies for PV storage systems in distribution grids," *IEEE Trans. Smart Grid*, vol. 5, no. 2, pp. 1002–1009, Mar. 2014.
[12] M. N. Kabir, Y. Mishra, G. Ledwich, Z. Y. Dong, and K. P. Wong, "Coordinated control of grid-connected photovoltaic reactive power and battery energy storage systems to improve the voltage profile of a residential distribution feeder," *IEEE Trans. Ind. Informat.*, vol. 10, no. 2, pp. 967–977, May 2014.
[13] M. Bahramipanah, R. Cherkaoui, and M. Paolone, "Decentralized voltage control of clustered active distribution network by means of energy storage systems," *Electr. Power Syst. Res.*, vol. 136, pp. 370–382, Jul. 2016.
[14] T. Morstyn, B. Hredzak, and V. G. Agelidis, "Control strategies for microgrids with distributed energy storage systems: An overview," *IEEE Trans. Smart Grid*, vol. 9, no. 4, pp. 3652–3666, Jul. 2018.
[15] A. A. Hamad, H. E. Farag, and E. F. El-Saadany, "A novel multiagent control scheme for voltage regulation in DC distribution systems," *IEEE Trans. Sustain. Energy*, vol. 6, no. 2, pp. 534–545, Apr. 2015.
[16] B. Zhang, A. Y. Lam, A. D. Dominguez-Garcia, and D. Tse, "An optimal and distributed method for voltage regulation in power distribution systems," *IEEE Trans. Power Syst.*, vol. 30, no. 4, pp. 1714–1726, Jul. 2015.
[17] Y. Wang, K. T. Tan, X. Y. Peng, and P. L. So, "Coordinated control of distributed energy-storage systems for voltage regulation in distribution networks," *IEEE Trans. Power Del.*, vol. 31, no. 3, pp. 1132–1141, Jun. 2016.
[18] M. Zeraati, M. E. H. Golshan, and J. M. Guerrero, "Distributed control of battery energy storage systems for voltage regulation in distribution networks with high PV penetration," *IEEE Trans. Smart Grid*, vol. 9, no. 4, pp. 3582–3593, Jul. 2018.
[19] R. Zhang and B. Hredzak, "Nonlinear sliding mode and distributed control of battery energy storage and photovoltaic systems in AC microgrids with time delays," *IEEE Trans. Ind. Informat.*, vol. 15, no. 9, pp. 5149–5160, Sep. 2019.
[20] C. P. Nguyen and A. J. Flueck, "Agent based restoration with distributed energy storage support in smart grids," *IEEE Trans. Smart Grid*, vol. 3, no. 2, pp. 1029–1038, Jun. 2012.
[21] S. Soman, K. Parthasarathy, and D. Thukaram, "Curtailed number and reduced controller movement optimization algorithms for real time voltage/reactive power control," *IEEE Trans. Power Syst.*, vol. 9, no. 4, pp. 2035–2041, Nov. 1994.
[22] D. T. Phan and X. A. Sun, "Minimal impact corrective actions in security-constrained optimal power flow via sparsity regularization," *IEEE Trans. Power Syst.*, vol. 30, no. 4, pp. 1947–1956, Jul. 2015.
[23] F. Dorfler, M. R. Jovanovic, M. Chertkov, and F. Bullo, "Sparsity-promoting optimal wide-area control of power networks," *IEEE Trans. Power Syst.*, vol. 29, no. 5, pp. 2281–2291, Sep. 2014.
[24] J. Mohammadi, G. Hug, and S. Kar, "A fully distributed cooperative charging approach for plug-in electric vehicles," *IEEE Trans. Smart Grid*, vol. 9, no. 4, pp. 3507–3518, Jul. 2018.
[25] J. F. C. Mota, J. M. F. Xavier, P. M. Q. Aguiar, and M. Puschel, "D-ADMM: A communication-efficient distributed algorithm for separable optimization," *IEEE Trans. Signal Process.*, vol. 61, no. 10, pp. 2718–2723, May 2013.
[26] J. F. C. Mota, J. M. F. Xavier, P. M. Q. Aguiar, and M. Puschel, "Distributed optimization with local domains: Applications in MPC and network flows," *IEEE Trans. Automat. Contr.*, vol. 60, no. 7, pp. 2004–2009, Jul. 2015.
[27] R. P. Costa, J. M. Lemos, J. F. C. Mota, and J. M. F. Xavier, "D-ADMM based distributed MPC with input-output models," in *Proc. IEEE Conf. Control Appl. (CCA)*, Oct. 2014, pp. 699–704.
[28] L. Xu, X. Ruan, C. Mao, B. Zhang, and Y. Luo, "An improved optimal sizing method for wind-solar-battery hybrid power system," *IEEE Trans. Sustain. Energy*, vol. 4, no. 3, pp. 774–785, Jul. 2013.
[29] M. E. Khodayar, M. Shahidehpour, and L. Wu, "Enhancing the dispatchability of variable wind generation by coordination with pumped-storage hydro units in stochastic power systems," *IEEE Trans. Power Syst.*, vol. 28, no. 3, pp. 2808–2818, Aug. 2013.
[30] L. Yu, D. Czarkowski, and F. De Leon, "Optimal distributed voltage regulation for secondary networks with DGs," *IEEE Trans. Smart Grid*, vol. 3, no. 2, pp. 959–967, Jun. 2012.
[31] G. Valverde and T. Van Cutsem, "Model predictive control of voltages in active distribution networks," *IEEE Trans. Smart Grid*, vol. 4, no. 4, pp. 2152–2161, Dec. 2013.
[32] *CISLResearchDataArchive*. Accessed: 2020. [Online]. Available: http://rda.ecar.edu/
[33] *Australia's Official Weather Forecast & Weather Radar Website*. Accessed: 2020. [Online]. Available: http://www.bom.gov.au/
[34] Y. Zhang, Y. Xu, H. Yang, Z. Y. Dong, and R. Zhang, "Optimal whole-life-cycle planning of battery energy storage for multi-functional services in power systems," *IEEE Trans. Sustain. Energy*, to be published.
[35] *20 Exciting Storage Products*. Accessed: Sep. 23, 2015. [Online]. Available: http://www.pv-magazine.com/fileadmin/PDFs/pv-magazineStorageSpecialJul2015.pdf

YONGXI ZHANG (Member, IEEE) received the B.E. and M.S. degrees in electrical engineering from the Changsha University of Science and Technology, Changsha, China, in 2008 and 2011, the M.S. degree in electrical engineering from The Hong Kong Polytechnic University, Hong Kong, in 2010, and the Ph.D. degree from the School of Electrical and Information Engineering, The University of Sydney, Sydney, Australia, in 2017.

She is currently a Lecture with the School of Electrical and Information Engineering, Changsha University of Science and Technology, Changsha, China. Her research interests include renewable energy, and power system operation and planning

KE MENG (Member, IEEE) received the Ph.D. degree in electrical engineering from the University of Queensland, Brisbane, QLD, Australia, in 2009. He is currently with the School of Electrical Engineering and Telecommunications, University of New South Wales, Sydney, NSW, Australia. He is also a Visiting Professor with the Changsha University of Science and Technology, Changsha, China. His research interests include power system stability analysis, power system planning, renewable energy, and power system data analytics.

FENGJI LUO (Member, IEEE) received the bachelor's and master's degrees in software engineering from Chongqing University, China, in 2006 and 2009, respectively, and the Ph.D. degree in electrical engineering from The University of Newcastle, Australia, 2014. He is currently a Lecturer and an Academic Fellow with the School of Civil Engineering, The University of Sydney, Australia. His research interests include energy demand side management, smart grid, smart building, and energy informatics. He has published over 100 articles in these areas. He receives the Pro-Vice Chancellor's Research and Innovation Excellence Award of The University of Newcastle, in 2015, the Australia-Japan Emerging Research Leader Award, in 2016, and the UUKI Rutherford Fellowship at the Future Energy Institute, Brunel University London, in 2018.

HONGMING YANG (Member, IEEE) received the M.S. degree in electrical engineering from Wuhan University, Wuhan, China, in 1997, and the Ph.D. degree in electrical engineering from the Huazhong University of Science and Technology, Wuhan, in 2003. She was a Research Associate with The Hong Kong Polytechnic University, from 2009 to 2010, a Visiting Scholar with North Carolina State University, from 2010 to 2011, and a Research Fellow with the University of Newcastle. She is currently a Full Professor with the Changsha University of Science and Technology, Changsha, China. Her research interests include power system analysis and power markets

JIAHUA ZHU received the B.E. degree in electrical engineering from the Changsha University of Science and Technology, Changsha, China, in 2019, where he is currently pursuing the master's degree with the school of Electrical and Information Engineering. His research interests include energy storage systems and second life batteries.

ZHAO YANG DONG received the Ph.D. degree from The University of Sydney, Australia, in 1999. He was a Ausgrid Chair and the Director of the Ausgrid Centre for Intelligent Electricity Networks (CIEN) providing R&D support for the 600M Smart Grid, Smart City national demonstration project. He also worked as a Manager for (transmission) system planning at Transend Networks (now TASNetworks), Australia. He is currently with the University of NSW (UNSW) Sydney, Sydney, Australia. He is also the Director of UNSW Digital Grid Futures Institute, and the Director of ARC Research Hub for Integrated Energy Storage Solutions. His immediate role is a Professor and the Head of the School of Electrical and Information Engineering, The University of Sydney. His research interests include smart grid, power system planning, power system security, load modeling, renewable energy systems, and electricity market. He has been serving/served as editor for several journals, including served as an Editor for the IEEE TRANSACTIONS ON SMART GRID, the IEEE TRANSACTIONS ON SUSTAINABLE ENERGY, the IEEE PES TRANSACTION LETTERS, and *IET Renewable Power Generation*. He is an international Advisor of the journal of *Automation of Electric Power Systems*.